

Cholinergic-related pupil activity reflects level of emotionality during motor performance

Marc Vidal^{1,2,3}  | Kelsey E. Onderdijk¹  | Ana M. Aguilera²  |
Joren Six¹  | Pieter-Jan Maes¹  | Thomas Hans Fritz^{1,3}  | Marc Leman¹ 

¹IPEM, Ghent University, Ghent, Belgium

²Department of Statistics and Operations Research, Institute of Mathematics, University of Granada, Granada, Spain

³Department of Neurology, Max Planck Institute for Human Cognitive and Brain Sciences, Leipzig, Germany

Correspondence

Marc Vidal, IPEM, Ghent University, B-9000 Ghent, Belgium.

Email: marc.vidalbadia@ugent.be

Thomas Hans Fritz, Department of Neurology, Max Planck Institute for Human Cognitive and Brain Sciences, 04103 Leipzig, Germany.

Email: fritz@cbs.mpg.de

Funding information

Flemish Government, Methusalem funding. FWO project, Grant/Award Number: G046518N; Consejería de Conocimiento, Investigación y Universidad, Junta de Andalucía (Spain), Grant/Award Number: A-FQM-66-UGR20; Spanish Ministry of Science and Innovation, Grant/Award Number: PID2020-113961GB-I00; IMAG-Maria de Maeztu, Grant/Award Number: CEX2020-001105-M/AEI/10.13039/501100011033

Edited by: John Foxe

Abstract

Pupil size covaries with the diffusion rate of the cholinergic and noradrenergic neurons throughout the brain, which are essential to arousal. Recent findings suggest that slow pupil fluctuations during locomotion are an index of sustained activity in cholinergic axons, whereas phasic dilations are related to the activity of noradrenergic axons. Here, we investigated movement induced arousal (i.e., by singing and swaying to music), hypothesising that actively engaging in musical behaviour will provoke stronger emotional engagement in participants and lead to different qualitative patterns of tonic and phasic pupil activity. A challenge in the analysis of pupil data is the turbulent behaviour of pupil diameter due to exogenous ocular activity commonly encountered during motor tasks and the high variability typically found between individuals. To address this, we developed an algorithm that adaptively estimates and removes pupil responses to ocular events, as well as a functional data methodology, derived from Pfaffs' generalised arousal, that provides a new statistical dimension on how pupil data can be interpreted according to putative neuromodulatory signalling. We found that actively engaging in singing enhanced slow cholinergic-related pupil dilations and having the opportunity to move your body while performing amplified the effect of singing on pupil activity. Phasic pupil oscillations during motor execution attenuated in time, which is often interpreted as a measure of sense of agency over movement.

KEYWORDS

emotional motor control, functional data, generalised arousal, neuromodulation, singing, turbulence

Abbreviations: ACh, acetylcholine; BF, basal forebrain; Ch, cholinergic; CWT, continuous wavelet transform; GA, generalised arousal; KL, Karhunen-Loève; LC, locus coeruleus; M, body sway to music; MS, body sway plus singing; NE, norepinephrine; NM, no movement only listening; NMS, singing but no body sway allowed; RMSE, root mean square error; ROE, responses to ocular events.

Thomas Hans Fritz and Marc Leman are last co-authors.

This is an open access article under the terms of the [Creative Commons Attribution-NonCommercial-NoDerivs](https://creativecommons.org/licenses/by-nc-nd/4.0/) License, which permits use and distribution in any medium, provided the original work is properly cited, the use is non-commercial and no modifications or adaptations are made.

© 2023 The Authors. *European Journal of Neuroscience* published by Federation of European Neuroscience Societies and John Wiley & Sons Ltd.

1 | INTRODUCTION

Optimal levels of arousal are critical for perceptual and cognitive functions, given that arousal modulates entire classes of responses to various events, for example, making an organism more responsive to sensory stimuli, more ready to execute voluntary motor activity and more emotionally responsive (Pfaff, 2009). Physiologically, regulation of arousal and autonomic function is related to the activity of the locus coeruleus norepinephrine (LC-NE) and basal forebrain cholinergic (BF-Ch) systems (Aston-Jones & Cohen, 2005; Benarroch, 2009, 2021; Berridge, 2008; Everitt & Robbins, 1997; Liebe et al., 2022; Sara, 2009). The LC-NE activity plays an important role in enhancing the processing of information salience (Vazey et al., 2018; Wang & Munoz, 2015) and has been shown to have an influence on decision making (de Gee et al., 2017; Duzel & Guitart-Masip, 2013). BF-Ch activity is a key component in promoting sensory perception (Pinto et al., 2013) and in emotion regulation (Ballinger et al., 2016; Bentley et al., 2003a, 2003b; McGaugh, 2004; Picciotto et al., 2012). Furthermore, its engagement is particularly characteristic as an integral aspect of motor activity, for example, during locomotion (Reimer et al., 2016), or other types of body movements independent of locomotion (Nelson & Mooney, 2016).

Prior studies in humans and non-human animals have demonstrated that, under isoluminance conditions, a causal relationship exists between pupil fluctuations and the activity in the LC and BF-Ch neurons (Breton-Provencher & Sur, 2019; de Gee et al., 2017; Joshi & Gold, 2020; Joshi et al., 2016; Murphy et al., 2014; Nelson & Mooney, 2016; Reimer et al., 2016). However, neuromodulatory mechanisms underlying movement control and their corresponding effects on pupil behaviour are not yet well-understood. Neurophysiological work in rodents has shown that the pupil tends to dilate concurrently with activity of the NE and Ch axons before locomotion onset (Reimer et al., 2014). This dilation is prolonged along with a sustained Ch axonal activity until motor offset, showing a hallmark latency to reach baseline levels (McGinley et al., 2015; Reimer et al., 2014; Vinck et al., 2015). BF-Ch inputs have also been related to microdilations induced by small body movements (Nelson & Mooney, 2016). NE phasic activity tracks transient and differential dilations during motor and passive states (Joshi et al., 2016; Reimer et al., 2016). A recent study has shown, however, that these projections are more likely to be related to infrequent and large dilation events, suggesting that inferencing on repeated measures could increase the accuracy of the NE axonal estimates (Megemont et al., 2022). Note that while arousal and motor activity have been shown to be to some degree

independent in how they modulate firing in cortical circuits (Vinck et al., 2015), their interplay seems to notably contribute to functional plasticity in the cortex, for example, enhancing learning (Albergaria et al., 2018).

The behaviour of BF-Ch and LC-NE systems in humans with respect to motor functionality and how it relates to pupillary changes has been less investigated. Nevertheless, several studies on visuo-motor tasks have reported that modulation of pupil size is dominated by the motor response rather than other cognitive factors; see Martin et al. (2020) and references therein. The intensity of physical exercise in the absence of visual cues has been previously associated with an increased baseline pupil diameter (Hayashi et al., 2010; Zénon et al., 2014), which, when performed with moderate intensity, was comparable with when participants performed mental arithmetic tasks (Hayashi et al., 2010). Subsequent studies have corroborated these findings using measures of peak oxygen consumption (\dot{V}_{O_2}) and minute ventilation (\dot{V}_E), further demonstrating that exercise-intensity-dependent pupil dilation was exponentially correlated to these physiological measures (Kuwamizu et al., 2022). Other studies have tested the effects of single bouts of exercise on cognitive inhibitory control as measured by pupillometry following the physical activity, suggesting that task enhancement was, to some degree, independent of LC-related pupil activity (McGowan et al., 2019; Shigeta et al., 2021). Instead, findings have shown that choline supplements for boosting cholinergic activation enhanced performance accuracy over velocity during visuo-motor aiming tasks, which translated into a relative decrease in pupil size compared with when movements were faster and less accurate (Naber & Murphy, 2019; Naber et al., 2015).

Here, we investigate the inverse problem of inferring the activity of brainstem arousal systems from a blinded-inference paradigm perspective, using pupil recordings in humans. We formulate a frequency-specific schema of analysis based on prior investigations on motor tasks in rodents (Reimer et al., 2016) that is determined by the structure of a musical piece. Our analytical methodology is motivated by the ‘generalised arousal’ (GA) hypothesis (Pfaff, 2009; Pfaff et al., 2008, 2012). Several components of the nervous system, such as the medullary reticular formation, thalamus and cortex, contribute to GA, which is crucial for initiation of any behaviour during arousal states. The relevance of nucleus gigantocellularis neurons, whose activity is related to serotonin and ACh, together with adrenergic projections from LC, have been reported to play a role in modulating GA (Calderon et al., 2016; Liu et al., 2016; Martin et al., 2011; Tabansky et al., 2018). Here, we assume that the confluence of these neural mechanisms makes the latent dynamics of pupil

activity a potential candidate to model GA function. The proposed methodology extends previous efforts of GA analysis to functional data (Ramsay & Silverman, 2005) through a reduction method that allows capturing variability in a population who sequentially performs different motor tasks in a musical context that are designed to vary in degree of emotional engagement.

Participants with musical training were recruited to perform under different movement conditions, to emotionally engage the performers in various degrees during their motor tasks. Four conditions were compared as follows: (i) no movement (NM), only music listening, (ii) body sway to music (M), (iii) singing but no body sway allowed (NMS), and (iv) body sway plus singing (MS). We hypothesise that actively engaging in musical behaviour while singing and moving along to the music will more strongly engage participants emotionally and lead to a qualitatively different pattern of tonic and phasic pupil activity. Given the relevance of GA for emotional motor control in the basal forebrain (Martin et al., 2011), we speculate that GA modelling of BF-ACh pupil-related activity might be a way of objectively quantifying emotional response, whereas transient fluctuations related to LC-NE activity occurring in parallel in higher subbands might reflect other cognitive parameters possibly related to attention.

2 | MATERIALS AND METHODS

2.1 | Participants

Fifteen participants (all female, aged 21–50), with formal and/or informal musical education (Mean = 11.46 years; SD = 6.51), gave written consent for taking part in the study, approved by the local ethics committee (Faculty of Arts and Philosophy, Ghent University). They were right-handed and had corrected to normal vision, normal hearing and were neurologically healthy. All participants were screened on their experience with singing in a choir, which ensured they had experience with singing a steady part in the presence of other voices. They received voucher credit for their participation.

2.2 | Acquisition of pupil data and other modalities

Pupil diameter was recorded at 30 Hz frequency rate using Pupil Lab's wearable headset with integrated cameras (Logitech C930e) directed towards the right eye. A force sensor platform with 59 cm radius was used to control for body movement. This platform consists of a plate

with four sensitive weight sensors underneath (one at each corner) to register variations in pressure related to body movement. Each sensor is captured with the 13 bit Analog Digital Converter of a micro-controller (Teensy 3.1, PJRC) at 120 Hz. The sensor data are wrapped into MIDI packets. This allowed for in sync recording of audio and sensor values using a standard digital audio workstation software (Ableton Live 9). The participant's singing voice was recorded with a Shure Beta 87A microphone. Next to this, a decibel metre (UNI-T UT352) was used to monitor and review the volume level before the start of the experiment (to limit the effect of loudness).

2.3 | Procedure and rating of perceived level of emotionality

The experiment was conducted in a dark room with steady LED luminance of less than about 30 cd/m² (Uni-T Luminometers UT381). The participants stood on the platform, facing three speakers at a distance of 2 m. During conditions NM and NMS, they had to stand still looking at a white cross placed on the middle speaker, whereas in conditions M and MS, gaze movement was allowed facing forward horizontally where the speakers were located. Gazing upwards or downwards was advised against. Five-point calibration and validation were performed before the start of the experimental session. Hereafter, we asked participants to stand on their assigned spot in the room and to sing the rehearsed melody by heart. This allowed us to check whether participants learned the melody to complete the various tasks with fluency. Participants performed with an instrumental music piece including a three-part vocal harmony. In conditions NMS and MS, they sang the middle voice from the three-part harmony, which was in the singing conditions not audible in the music presentation (only their own voice could be heard to sing this part). The trial order was randomised. For further details concerning the experimental setting and stimuli, see supporting information (Video S1).

After performing each task, participants were asked to rate their perceived level of excitement and absorption (degree of correspondence with the activity) on a Likert scale from 1 'low level' to 7 'high level'. We used the terms absorption and excitement as attributes of positive emotionality.

2.4 | Analysis of the singing performance

Recordings of the singers were evaluated by two experts with more than 20 years of musical training and

teaching experience in musical institutions. They were asked to rate on a scale from 1 (very inaccurate) to 10 (very accurate) the following items: intonation, rhythm and fluency (smoothness of the performance, as in Nusseck and Wanderley (2009)). The recording files were blinded and randomised before their presentation to the evaluators. Furthermore, acoustic similarity between NMS and MS conditions was measured with the singing part isolated from the instrumental by calculating cosine similarity and Pearson's correlation on spectrogram-like representations (frequencies were in Mel).

2.5 | General data preprocessing and statistics

Outlying data produced by blinks taking values of zero (or close to it) were removed from 100 ms before until 200 ms after the observation ($6.962\% \pm 6.158$ of missing data). As an alternative to interpolate the removed values, we imputed them using an algorithm based on a vector autoregressive model with heavy-tailed Student's t distributed innovations that is robust against outliers (Zhou et al., 2020). This procedure reconstructs the missing data using stochastic parameters amenable for heavy-tailed and sparse high-dimensional data. Subsequently, the pupil time series were mean-centered and normalised to unit variance. Standardisation across subjects allowed to control for differential sensitivity to the ambient luminance, as to compute higher-order moments. Unless otherwise stated, the median pupil size of the interval from 200 ms to the start of the auditory stimuli was used as baseline. Similarly, the data recorded with the force platform were downsampled at 30 Hz, low-pass filtered (1.5 Hz) and normalised. To express this data as dynamic firing rates, we calculated the first derivative and its Hilbert envelope or instantaneous amplitude.

All data and statistical analyses were performed using custom-made R scripts (R Core Team, 2021) (ver. 4.2.0). Statistical significance was measured against an alpha level of 0.05.

2.6 | Estimation of cognitive-related pupil activity

Turbulent-like dynamics can be encountered in many physiological phenomena, such as in cardiac (Schmidt et al., 1999) or brain imaging signals (Deco & Kringelbach, 2020; Escrichs et al., 2022). In the current research scenario, it can be understood as chaotic

dynamics that appear as a distortion of a more parsimonious state by various physiological parameters. More precisely, in pupillometry, turbulence is observed after changes in retinal illuminance (e.g., when blinking), as the pupil tends to rapidly constrict and redilate transiently to tonic levels, drawing the shape of a negative gamma function in the signal (Figure 1a,e). Luminance-related changes directly modulate the feedforward response of V1 (striate cortex) that is independent of psychological factors like attentional load (Bombeke et al., 2016), suggesting that changes in pupil size due to autonomic regulation also affect visual perception to some degree. Note that while blinks are often considered informative of attentional or other arousal states (Demiral et al., 2023; Kawashima et al., 2022; Schwabe et al., 2011), their effect on pupil size is probably rather related to basic visual function.

Pupil responses produced by subtle changes in luminosity can act as confounders, notoriously biasing the results of a subsequent data reduction (Knappen et al., 2016; Yoo et al., 2021). The intensity, duration and frequency of pupil occlusion, together with abrupt visual changes resulting from movement, can generate turbulent flows in the signal hampering estimation of pupil behaviour related to cognitive processes. We observed that blinks are more likely to occur during movement and vocalisation tasks compared with the control task NM ($P < 0.05$ using permutation test for location based on means applying the Box-Cox transformation; see Christensen and Zabriskie (2021)), which is consistent with previous findings reporting an increasing blink rate due to complex motor activity during speaking (Brych et al., 2021). Furthermore, responses to ocular events (ROE) might overlap with other ROE in such conditions, which can lead to a nonlinear distortion of the signal. Taking all this into account, a systematic correction of ROE is necessary to provide reliable results about levels of pupil-linked arousal.

To detect these turbulent flows, we applied a novel unsupervised algorithm that accounts for slow and high-frequency ocular responses. The model uses nonlinear internal vector spaces of the pupil signal reconstructed by a third-order Butterworth band-pass filter with a fixed higher cutoff frequency and variable low-pass frequency cutoff to gradually remove localised abnormal oscillations.

2.6.1 | ROE reduction algorithm

Let $x_1, x_2, \dots, x_t, \dots, x_n$ be a univariate time series of n pupil diameter measurements and denote by $\text{BP}_{\omega, \bar{\omega}}(\cdot)$ a battery of third-order band-pass Butterworth filters with fixed

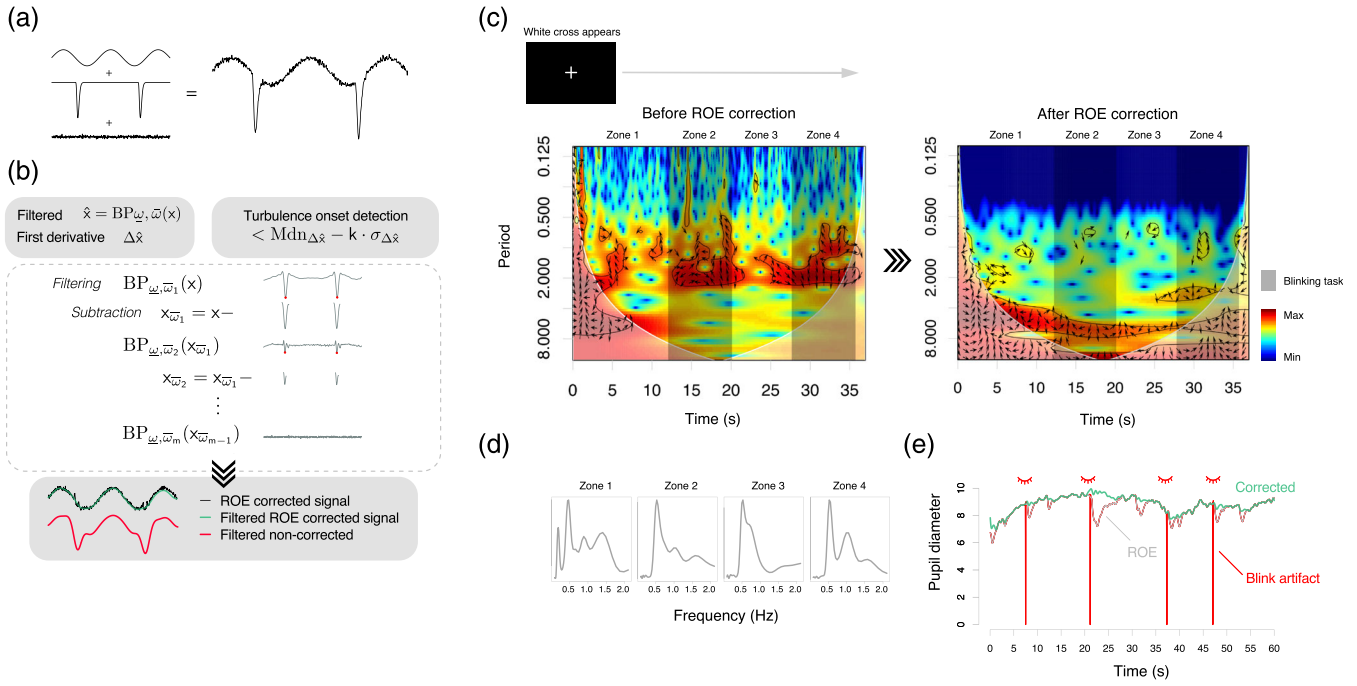


FIGURE 1 Removal of responses to ocular events (ROE): toy simulation and real data examples showing how the ROE algorithm works. (a) Simulated contaminated pupil data. (b) Downwards oscillations corresponding to ROE are detected using a battery of band-pass filters and progressively removed at each smoothing step subtracting the area of the curve generated below the nearest low-peak of the oscillation period to the turbulence onset (in red). (c) Continuous wavelet transform (CWT) before and after the application of the ROE correction (with final low-pass filter at 1.6 Hz). Zones shaded in grey depict the ROE phase changes during the blinking task (four blinks) with contours enclosing turbulent flow fields (regions with a significance level $>0.95\%$ according to a χ^2 test). (d) Series showing the row sums of the matrix containing significance levels of the CWT for the different zones marked in the power spectrum before ROE correction. (e) Application of the algorithm (with $k = 3$) to real data retrieved from the Python package FIRDeconvolution (Knapen & Gee, 2016)

cutoff frequency $\underline{\omega}$ and variable low-pass frequency cutoff $\bar{\omega}_j$ ($j = 1, \dots, m$). Then, the ROE reduction consists in the following iterative process.

For each filtering step $\bar{\omega}_j$, we repeat the following:

1. Calculate $\hat{x}_t = \text{BP}_{\underline{\omega}, \bar{\omega}_j}(x_t)$ and determine the set of turbulence onsets t_{τ_l} ($l = 1, \dots, L_j$) such that $\Delta \hat{x}_{t_{\tau_l}} < \text{Mdn}_{\Delta \hat{x}} - k \cdot \sigma_{\Delta \hat{x}}$, where Δ denotes the differencing operator and k is a dispersion hyperparameter.
2. For each t_{τ_l} at the j th filtering step, let $\{t_{a_l}, \dots, t_{\tau_l}, \dots, t_{p_l}\}$ be the set of observed time points where t_{a_l}, t_{p_l} represent the index positions related to the smallest nearest neighbouring peak of $\hat{x}_{t_{\tau_l}}$ and the relative position of this peak before or after t_{τ_l} . Then, the subtraction can be performed using baseline correction as

$$(x_{t_{a_l}:t_{p_l}} - x_{t_{a_l}}) - (\hat{x}_{t_{a_l}:t_{p_l}} - \hat{x}_{t_{a_l}}) + x_{t_{a_l}},$$

where $x_{t_{a_l}:t_{p_l}}$ is the snippet containing the ROE.

3. Update x_t for each τ_l and then go to the next filtering step.

2.6.2 | Parameter selection and validation

To determine the parameters $\underline{\omega}, \bar{\omega}_j, k$, we recorded a participant who was asked to blink four times synchronised with an auditory beat (of 2 s duration) in two time frames separated by pauses. The beat appeared four times with a different sound during the pauses to alert the participant of the beginning/end of the blinking task. Blinks were intentionally performed longer to see their effect on the signal. During the pauses, eventual and faster blinks also occurred. We recorded pupil activity in a dark environment where a white fixation cross was projected during the experiment. This produced a slow ROE related to changes in the luminance level (Figure 1c). For further details, see the Github repository in the data availability statement.

The continuous wavelet transform (CWT) (Morlet wavelet) was performed on the data to examine the pseudo-frequency scales characterising the dynamics of turbulence produced by ROE. Time-power spectra bias-corrected (Liu et al., 2007) and levels of significance (χ^2 test; see Torrence and Compo (1998)) are shown in Figure 1c. The ROE algorithm was applied in two steps from the baseline frequencies $\underline{\omega}_1 = 0, \underline{\omega}_2 = 0.25$ and $\bar{\omega}_{1,j} =$

(0.03, 0.045, ...), $\bar{\omega}_{2,j} = (0.5, 0.515, \dots)$ that allowed to detect slow and rapid ROE, respectively. We chose ω_2 guided by the CWT results analysing the series obtained by summing the values of each row of the matrix containing significance levels (zone 1, Figure 1d). The minima found (0.278 Hz) after the first local maximum (0.175 Hz), which roughly delimits the upper frequency range for the low-frequency ROE observed in zone 1, served as a point of reference. The value of $\omega_{1,1}$ was determined by Reimer's top frequency threshold for the slow ACh activity and $\omega_{2,1}$ again summing the values of each row of the matrix containing significance levels but now selecting the second peak of frequency (~ 0.5 Hz) which was noticeable across all zones analysed with blinking activity whether voluntary or not. The m th values of the $\bar{\omega}_j$'s vectors can be chosen based on a frequency limit above which pupil activity is rarely attributable to physiological sources (i.e., 4 Hz as suggested in Peysakhovich et al., 2015, and Knapen et al., 2016). Lastly, the corrected pupil data can be low-pass filtered at 4 Hz or at lower frequencies for subsequent analyses (we used 1.6 Hz; see Figure 1c).

The dispersion hyperparameter (k) from the filtered signal's first derivative median value is fixed to identify the abnormal oscillatory changes. Because blink responses contribute more variance to the signal in movement-controlled conditions (Knapen et al., 2016), a lower value than $k=3$ (which is often conventionally used) provided more realistic estimations. Thus, for ω_2 we modelled the dispersion hyperparameter as the decreasing exponential function $k=3 \cdot e^{-b}$, where b denotes the participants' blink rate. The turbulence onset is then defined as a low peak of velocity that surpasses the established dispersion threshold.

Application of the ROE algorithm to the data and other external data (Figure 1c,e) shows that the algorithm is capable to identify all ROE turbulence right after the blink artefact and also others that occur directly after ROE indistinctly of the artefact benchmark, possibly due to autonomic regulation (McDougal & Gamlin, 2015). More research is needed to refine parameter selection, for example, in different or even variable luminosity conditions assessed by multiple recording devices.

2.7 | Hilbert space modelling of generalised arousal function

2.7.1 | Fourier basis approximations of slow BF-Ch pupil-related activity

Axonal projections from the cholinergic neuromodulatory neurons during locomotion have been found to be

coherent with pupil oscillations in low frequencies (< 0.03 Hz) (Reimer et al., 2016). These frequencies operate on a timescale beyond what is often described as moment-to-moment changes/fluctuations; therefore, we examined pupil data across the duration of the entire musical excerpt. To characterise cholinergic activity through pupil measurements, in a first step, pupil curves are regressed out as smooth functions using a Fourier basis. The choice of a Fourier basis instead of other systems (B-splines, Wavelets) is supported by the assumption that the shape of the pupil is a perfect circle as well as the apparent periodic behaviour of the data. The dimension of the basis was selected in order to minimise the root mean square error (RMSE) between the observed data and the evaluated Fourier basis approximation (discrete predicted values). To shape the baseline modulations of interest, we selected the basis dimension on a low range ($p < 11$). This allowed to find a RMSE trade-off between middle- and low-frequency rhythmicity, notably reducing oscillatory activity (> 0.05 Hz; see Figure 2d) to levels of coherency previously found (Reimer et al., 2016).

2.7.2 | Fourier basis approximations of phasic LC-NE pupil-related activity

To quantify variations of noradrenergic activity through pupil diameter, we bandpass-filtered the data from 0.06 to 1 Hz (θ_1). This frequency band includes part of Reimer's subband for NE axonal activity (0.03–0.4 Hz) and ranges upwards with the high-frequency threshold determined in a recent study in humans (Montefusco-Siegmund et al., 2022) that is based on previous research in rodents (McGinley et al., 2015; Reimer et al., 2014). Above 1 Hz, results might be more accurately quantifiable in a more fine grained time scale. Note, however, that human pupillary oscillations in higher subbands have been linked to luminance effects rather than other cognitive factors (Naber et al., 2013; Peysakhovich et al., 2015).

Crucially, we are interested in representations of the pupil data less susceptible to baseline effects, as activity in noradrenergic projections in cortex, which is characterised by localised bursts, tracks phasic changes in pupil diameter with an observable causal effect on the pupil size gain (Joshi et al., 2016; Megemont et al., 2022; Reimer et al., 2016; Vazey et al., 2018). Therefore, we selected a high-pass cutoff of 0.06 Hz to ensure certain degree of stationarity, while also preventing overlap with slow BF-Ch pupil-related activity. To this end, we further propose a form of deconvolution by narrowbanding the signal into two additional subbands, from 0.2 to 1 Hz (θ_2) and from 0.4 to 1 Hz (θ_3). This technique is used as an alternative to taking first differences, which although it

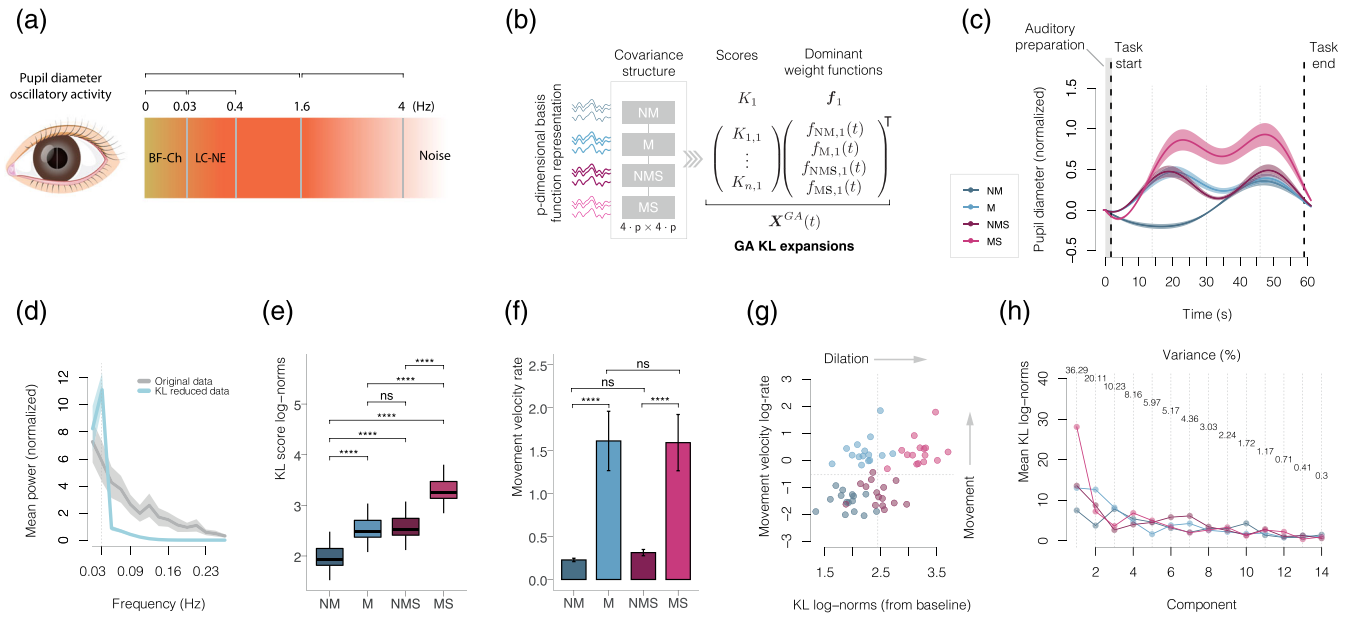


FIGURE 2 Neuromodulatory modelling of pupil data. (a) Schematic showing the division of the pupil signal in two frequency bands (0–1.6 and 1.6–4 Hz) as proposed by Peysakhovich and levels of coherency found by Reimer for the cholinergic axons (<0.03 Hz) and noradrenergic axons (0.03–0.4 Hz). Note that locus coeruleus norepinephrine (LC-NE) pupil-related activity (in red) is generally not restricted to values in the band 0.03–0.4 Hz. (b) Functional data model of Pfaff’s generalised arousal applied to the data. The model is based on one-factor (dominant eigenfunctions) Karhunen–Loève (KL) representation, estimated from a multivariate functional principal component analysis. (c) KL mean curves representing basal forebrain cholinergic (BF-Ch) pupil-related activity during the performance task. The grey dashed lines delimit section changes (see Figure 3a). (d) Spectral analysis comparing the original dataset to the KL reduced curves. (e) Comparison of baseline pupil rates of the KL curves for each condition (L^2 log-norms). (f) Comparison of force sensor platform velocity rates derived from the computation of the instantaneous amplitude via Hilbert transform (see Section 2). (g) Baseline pupil rates are plotted as a function of the platform velocity rates; the dashed lines represent the means for each group. (h) Means of the KL pupil rates for GA component and specific arousal forms $\{K_2f_2(t)\dots K_n f_n(t)\}$. A higher velocity decay in mean rates is observed in NMS and MS compared with the other conditions. Error bands were calculated at a 95% bootstrap confidence interval. Statistical comparisons were made using the Wilcoxon signed-rank test (with Bonferroni–Holm correction for multiple comparisons): * $P < 0.05$, ** $P < 0.01$, and *** $P < 0.001$; **** $P < 0.0001$; n.s., not significant. The error bars indicate standard errors.

has previously allowed to establish a number of correlations with NE axonal activity (Joshi et al., 2016; Reimer et al., 2016), after a first normalisation of the pupil data, statistical effects are more unlikely to survive when differentiating (which is also a kind of normalisation); see Discussion in Vidal and Aguilera (2023).

To enhance the functional representations of the data filtered above 0.06 Hz given their high density rhythmicity, we cut the data into four parts according to the formal structure described in Figure 3a. In order to accurately represent the shape of the rapid oscillations that were observed, we fitted a standard Fourier basis with a larger dimension ($p = 19$). Since the filtered curves tend to be rather stationary when slow oscillations are reduced ($P < 0.01$ on 83.88% of the data, augmented Dickey–Fuller test), the pupil series were mean-corrected instead of baseline aligned. [Correction added on 20 May 2023, after first online publication: The header for section 2.7.2 contained a typographical error and has been corrected in this version.]

2.7.3 | Multivariate functional GA model of pupil data

Within this setting, we resort to Pfaff’s GA form, an elementary form of arousal we denote by A_1 is expressed in combination to other specific forms A_2, \dots, A_n as

$$\text{Arousal} = F(K_1A_1 + K_2A_2 + \dots + K_nA_n), \quad (1)$$

where F is a mapping (non necessarily linear) and K_1, K_2, \dots, K_n are scores reflecting traits of the individual (Pfaff, 2009). Equation (1) can also be expressed dynamically as a differential equation (Calderon et al., 2016). Statistically, we interpret Equation (1) by means of a multivariate functional principal component analysis (MFPCA), which takes into account response dependencies through the pairwise cross-covariance functions (Acal et al., 2021; Jacques & Preda, 2014). This modelling strategy naturally extends previous linear formulations of

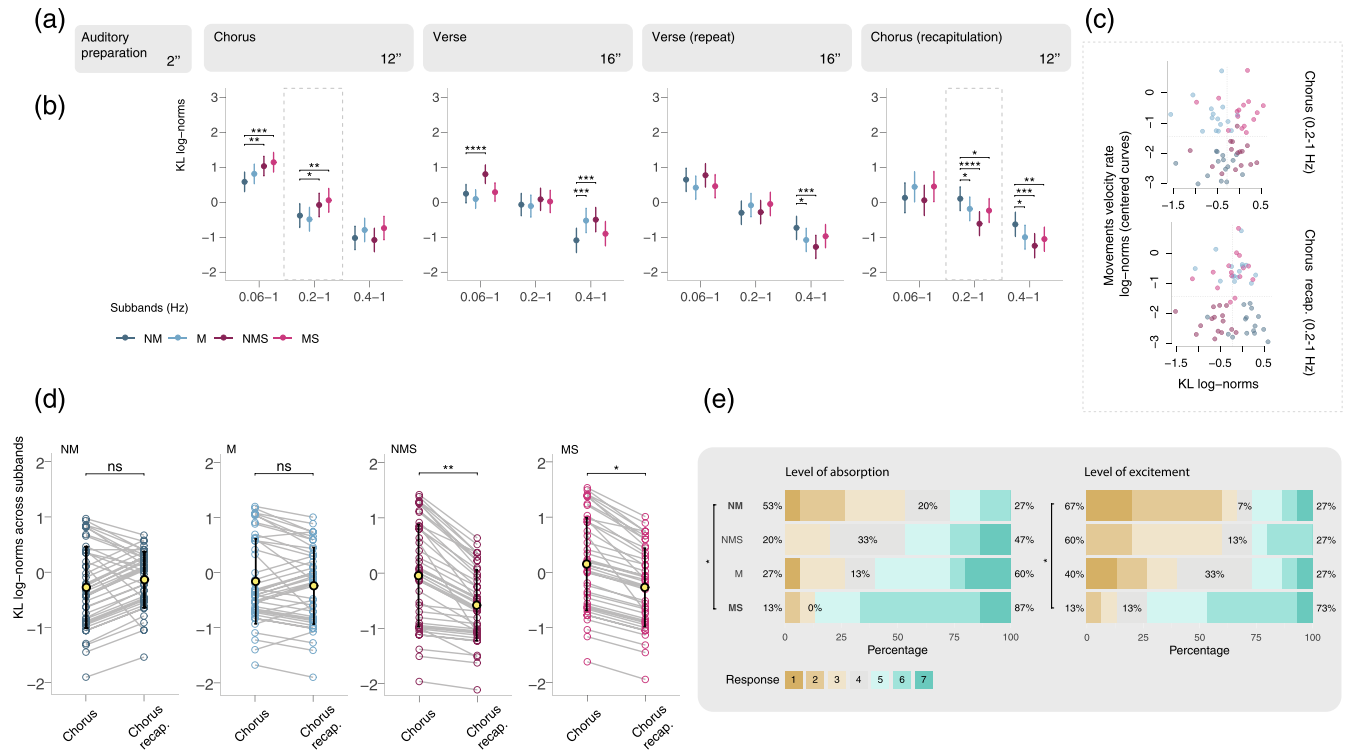


FIGURE 3 Modelling of locus coeruleus norepinephrine (LC-NE) activity (rapid pupil fluctuations) and behavioural data. (a) Schematic summarising the formal structure of the musical piece. (b) Comparison of generalised arousal (GA) pupil rates across different frequency subbands related to LC-NE activity. Statistical significance is measured as detailed in Figure 2 with respect to the no movement (NM) condition. Bars represent standard deviations. (c) Phasic pupil rates in the subband 0.2–1 Hz are plotted as a function of the locomotor activity (force sensor platform velocity rates). The dashed lines represent the means for each group. (d) Pooled dilation rates across all subbands ranging from 0.06 to 1 Hz. Statistical tests were conducted using the two sided Wilcoxon signed-rank test for single comparisons ($P < 0.05$ effects at MS were lost for multiple testing when using Bonferroni–Holm correction). (e) Perceived emotional attributes. Comparisons were made using Wilcoxon signed-rank test with Bonferroni–Holm correction.

the problem (Garey et al., 2003; Quinkert et al., 2011) to the functional case. In our approach, however, K_1 is a vector of scores obtained from the projection of the original functional data onto a vector of weight functions (one for each condition) with a major variance contribution. The GA we define in this context is then the set of random functions $\mathbf{X}^{GA}(t) = K_1 \mathbf{f}_1(t)$, where \mathbf{f}_1 is a vector of weight functions and \mathbf{X}^{GA} is a one-factor representation of the original data (see Figure 2b) also known as the truncated Karhunen–Loève (KL) expansion. One can say that the proposed model of dominant collective behaviour bears some resemblance to second-order models of criticality (Calderon et al., 2016; Sánchez-Islas et al., 2021).

Next, we formalise the above interpretation of Pfaff's GA model. We assume that the pupil data have been approximated by a finite linear combination of nonlinear Fourier functions (see, e.g., Ramsay and Silverman (2005)). Consider a sample of multivariate functional observations over a closed interval,

$$\mathbf{X}_i(t) = (X_{i1}(t), \dots, X_{iH}(t))^T; (i = 1, \dots, N; t \in [0, T]),$$

containing the pupillometric curves of N individuals in H experimental conditions. These functional approximations have the basis expansion $\mathbf{X}_i(t) = \Phi(t) \mathbf{c}_i^T$, where $\Phi(t)$ is a diagonal matrix of p dimensional vector valued Fourier functions with dimension $H \times (p_1 + p_2 + \dots + p_H)$, that is,

$$\Phi(t) = \begin{pmatrix} \phi_{11}(t) & \dots & \phi_{1p_1}(t) & 0 & \dots & 0 & \dots & 0 & \dots & 0 \\ 0 & \dots & 0 & \phi_{21}(t) & \dots & \phi_{2p_2}(t) & \dots & 0 & \dots & 0 \\ \vdots & & \vdots & \vdots & & \vdots & & \vdots & & \vdots \\ 0 & \dots & 0 & 0 & \dots & 0 & \dots & \phi_{H1}(t) & \dots & \phi_{Hp_H}(t) \end{pmatrix},$$

and $\mathbf{c}_i = (c_{i11}, \dots, c_{i1p_1}, c_{i21}, \dots, c_{i2p_2}, \dots, c_{iH1}, \dots, c_{iHp_H})$, its vector of coefficients. If all coefficients c_i are pooled together by rows, we can rewrite the above expression as $\mathbf{X}(t) = \mathbf{C} \Phi^T(t)$. The MFPCA is then obtained by solving the eigenequation

$$\Phi(s)\Sigma_C\mathbf{G}\mathbf{b}_m^\top = \lambda_m\Phi(s)\mathbf{b}_m^\top,$$

where $\Sigma_C = \frac{1}{n}\mathbf{C}^\top\mathbf{C}$, $\mathbf{G} = \int_{\mathcal{T}}\Phi(t)^\top\Phi(t)dt$ and \mathbf{b}_m^\top is the vector of coefficients of $\mathbf{f}_m(t) = \Phi(t)\mathbf{b}_m^\top$, a vector of weight functions obtained from the spectral decomposition of the variance-covariance function $\Gamma(s,t) = \Phi(s)\Sigma_C\Phi^\top(t)$ and $\lambda_m \in \mathfrak{R}$ its associated eigenvalues. [Correction added on 20 May 2023, after first online publication: The previous function has been updated to add a missing symbol in this version.] This problem has the algebraic solution in the matrix eigenproblem $\Sigma_C\mathbf{G}\mathbf{b}_m^\top = \lambda_m\mathbf{b}_m^\top$, where \mathbf{b}_m is in turn the eigenvector of the matrix Σ_C provided that \mathbf{G} is the identity matrix. This way, the principal component scores are $K_{im} = \mathbf{c}_{im}^\top\mathbf{b}_m$ and the corresponding KL expansion for the GA component is $\mathbf{X}_i^{GA}(t) = \boldsymbol{\mu}(t) + K_{i1}\mathbf{f}_1(t)$, where $\boldsymbol{\mu}(t)$ is a vector of mean functions of $\mathbf{X}_i(t)$ and $\mathbf{f}_1(t)$ is a vector of eigenfunctions (one per condition). Specific forms of arousal are then similarly obtained as

$$\{\mathbf{X}_i^{(2)}(t) = \boldsymbol{\mu}(t) + K_{i2}\mathbf{f}_2(t), \dots\}.$$

Note that the MFPCA is reduced to the multivariate PCA of the Fourier coefficients concatenated across trial conditions within each subject.

As the MFPCA (or second-order models) are based on a Gaussian assumption, some unusual observations might significantly influence the estimation of the covariance and the quality of the estimators of its spectrum. Therefore, prior to application of the method, we checked whether this assumption was satisfied. After ROE removal, no multivariate functional outliers were detected (Arribas-Gil & Romo, 2014), meaning that these dominant dynamics we retrieved from our data are robust and consistent for inferencing. Computational implementations of the MFPCA can be found in the R packages `fda`, `funHDDC` and `MFPCA`.

3 | RESULTS

3.1 | GA levels of pupil-related low-frequency cholinergic function change with emotionality of motor performance

The MFPCA of the smoothed pupil data reported a 36.29% of explained variance for the GA component, which has previously been reported to account for less than half of the variance (Calderon et al., 2016). Levels of GA were quantified by calculating the L^2 log-norm (from the baseline) of the KL curves. We found higher dilation rates of tonic

activity in all motoric conditions compared with NM (Figure 2e), with MS leading to a significant increase compared with the other conditions. By contrast, no differences were found between the pupil dilation rates of M and NMS, despite levels of motor activity being highly differentiated (Figure 2f,g). Motor activity rates (at least in terms of body sway) did not differ between M and MS.

3.2 | Amplitude of sensorimotor engagement determines change in LC-related pupil behaviour during chorus recapitulation

It can be argued that the human fascination with music to a great degree relates to music's capacity to dynamically vary expectation (Koelsch et al., 2019). A systematic variation of such aspects of stimulus property over time is an inherent quality of the stimulus material used in the present study. Accordingly, we looked at LC-related pupil behaviour in relation to musical structures that are known to systematically influence expectations: verse and chorus (Figure 3a). This also corresponds to predictive coding theories (Auksztulewicz & Friston, 2016; Friston & Kiebel, 2009) that state that the brain is a solver of likelihood functions, leading to the neuronal codes that predict sensory perception, so that cognitive processing is influenced by previous exposure. Accordingly, we investigated if pupil indices are modulated with chorus recapitulation.

We used Pfaff's GA formula for MFPCA reduction, although now applied to each part of the musical structure. Dominant fast and transient dilations can be seen as GA approximations in a lower time scale. Pupil behaviour differences between chorus and chorus recapitulation were observed. As shown in Figure 3b, an overall decrease in pupil dilation was found during the movement conditions along the different parts of the formal structure. A higher level of dilation was observed in the singing conditions during chorus and first verse compared with NM, which was significantly higher for θ_1, θ_2 during the chorus. In the recapitulation, M, NMS and MS were more prominently lowered in θ_2, θ_3 . This is apparent in the scatterplots (Figure 3c), where the singing conditions shifted left in the axis of the KL log-norms as a function of the velocity rate measured with the movement sensors. We also found evidence of this pupil constriction in a post hoc analysis testing differences across subbands by pooling all scores of each respective chorus part as a single variable. Results suggest a general decrease of dilation indices in NMS and MS (Figure 3d). No significant differences were reached in M and NM.

3.3 | Behavioural data

The discrepancy between the two experts' evaluations of the singer's performance was small ($T^2 = 1.922$, $P = 0.094$), and differences between the singing conditions were not significant ($T^2 = 1.062$, $P = 0.396$). The averages across conditions of each item to be evaluated were generally high (intonation: NMV = 8.333 ± 1.582 , MV = 8.566 ± 1.006 ; rhythm: NMV = 9.466 ± 1.008 , MV = 9.6 ± 0.723 ; fluency: NMV = 9.233 ± 0.971 , MV = 9.466 ± 0.571). The analysis contrasting the voice recordings between the NMV and MV conditions shows that the quality of the performance in both conditions was similar (cosine similarity: 0.97 ± 0.01 ; Pearson's correlation: 0.87 ± 0.05 — means and SDs across participants using a suitable score transformation). [Correction added on 20 May 2023, after first online publication: The previous sentence has been updated for clarity in this version.]

Participant's subjective ratings of the level of excitement and absorption (Figure 3e) show that a significant percentage of participants had a higher emotional experience when singing and moving along to the music compared with when they were only listening ($P < 0.05$, using Wilcoxon signed-rank test with Bonferroni–Holm correction).

4 | DISCUSSION

Musical activities are known to readily evoke emotional experiences and singing, as well as other expressive vocalisations, can often be regarded as a rather intense emotional activity (Frühholz et al., 2014; Giordano et al., 2021; Holstege & Subramanian, 2016; Scherer et al., 2017; Schwartz et al., 2022). Body movement and sway have been described to happen automatically during intense musical engagement (Chang et al., 2017; Leman, 2016), possibly through so-called empathic gestural attuning (Leman, 2008), where musical features such as beat, rhythm, melody and timbre may trigger body gesture associations. A recent EEG study reported enhanced mu activity on a left hemisphere mu cluster during music listening while having to remain still, which has been argued to possibly correspond to motor inhibition of the natural incline to move to music (Ross et al., 2021). Introducing additional constraints on physical movement is often compulsory in Western classical professional musicians, and it also demonstrates to the audience an enhanced control that is perceived as an attribute of professionalism. Very relevant for the current study design, using musical engagement allowed for experimentally structuring the investigation of emotionality. At the same time, introducing the requirement to inhibit body sway during the task,

more specifically, singing while additionally having the constraint not to move along and sway, allowed for less emotional experience of the performer than singing while being allowed to move freely with the body.

Our analyses suggest that inhibition of body sway during singing results in an enhanced pupil baseline tone that is comparable with when participants did not sing but only swayed along to the music. It might be that, for a musician, synchronising with either voice or body engages similar cognitive processes to a comparable degree and that engaging in synchronisation of both voice and body sway does combine to a different quality of immersive and emotional experience. This corresponds to the behavioural findings showing higher level of emotionality during MS. Notably, participants performed singing with a similar quality with and without body sway as assessed by evaluators, supporting the notion that the observed differences were indeed due to differences in emotionality and not to other parameters such as task difficulty. Current analyses rather show that cognitive load corresponds to values of LC-NE subbands (Figure 3b, chorus), where singing led to an increased pupil rate compared with non-singing conditions. No differences were found between pupil rates in conditions NMS and MS, which reflects participants' musical proficiency and further supports this interpretation of the results.

Following the discussion in Reimer et al. (2016), a modulation of slow frequency cholinergic activity and related pupil activity could be associated with pre-motor planning, arousal or both. While certainly controlling only voice and controlling body sway correspond to an involvement of different somatotopically organised pre-motor representations (Lévêque & Schön, 2015) and selective neural populations in the auditory cortex (Norman-Haignere et al., 2022; Staib & Frühholz, 2021), their effect in terms of pupil activity is comparable (Figure 2e). This rather seems to indicate that the cholinergic associated pupil activity reflects arousal level. As shown in Figure 2c, the level of pupil dilation increases from no movement during music listening to singing while not moving along to the music, to singing while moving along to the music. Given that arousal is a consistent dimension of emotion in arousal models and musical activities readily evoke emotion, we argue that in this musical context, a variation of action as part of musical tasks systematically varies level of emotionality. Research in support of this hypothesis shows that cholinergic activity contributes to emotion regulation (Ballinger et al., 2016; Bentley et al., 2003a; 2003b; McGaugh, 2004) during diverse musical and motor experiences (Blood & Zatorre, 2001; Jaffe & Brainard, 2020; Koelsch, 2014). We are aware that performing different

motor acts (e.g., singing or swaying), involves a different set of physiological resources that correspond to a different set of neural activation patterns that cannot solely be regarded as emotional. However, from the perspective of our knowledge on a dichotomy of voluntary and emotional motor control (Holstege & Subramanian, 2016; Holstege et al., 1996), we know that movement and emotionality are entwined. The current findings on the variability of the slow pupil dynamics are therefore congruent with the GA hypothesis and related theories on the emotional motor system which associate mitigation of emotional cues with action (Martin et al., 2011).

Musical structure and musicians' sway during performance has been previously described to covary systematically (Demos et al., 2018). Because body sway was one major aspect of the task, we took into account the formal structure of the musical piece when investigating the time-course of pupil dilation. Furthermore, pupil behaviour in relation to musical structure is applicable to understand rapid pupil fluctuations (0.06–1 Hz) that have been observed to relate to LC activity, which is often modulated during changes in stimulation, especially if such changes relate to the task. We observed that the pupil first dilated and then attenuated over time and repetition of the music. Larger and rapid pupil dilations have been associated to cortical desynchronisation (suppression of low-frequency fluctuations), a form of attentional state required to accurately process sensory information (Harris & Thiele, 2011; McGinley et al., 2015; Vinck et al., 2015), also in the auditory domain (Pachitariu et al., 2015; Sakata, 2016). Although this pattern of dilation and posterior attenuation when musical sections repeated was apparent in all motor conditions (Figure 3b), it was particularly robust during the singing conditions as shown in our post hoc analyses (Figure 3d). Such attenuation might correspond to the pupil's ability to respond to information from dynamic environments, possibly reflecting a process of active inference (Koelsch et al., 2019) in musical performance, even when visual information is controlled for. Pupil activity in correspondence to multimodal cognitive (rather than visual) processing has previously been shown. For example, higher learning rates in a prediction task were associated with a smaller baseline pupil diameter (Nassar et al., 2012) or biases on subject's internal beliefs related to higher pupil dilation in dynamic environments (Filipowicz et al., 2020; Krishnamurthy et al., 2017). In addition, motor engagement during performance seems to enhance this aspect of pupil activity given that attenuation of LC-related pupil indices occurs mainly during motor conditions as shown in our analyses (Figure 3b,d). Similar results have also been

reported during motor tasks, reflecting motor control and learning (Naber & Murphy, 2019; White & French, 2017).

Furthermore, we have introduced an unsupervised algorithm that allows to detect ROE of different duration and amplitude regardless of the artefact benchmark. The method works in a nonlinear fashion, which makes it suitable for non-stationary environments and only recasts on a dispersion parameter that can be relaxed according to the levels of contamination. Turbulence due to ROE is then minimised, providing a more precise estimate of the neurological processes under investigation. With this, dissociable traits in the pupil behaviour related to the LC and BF-ACh activity found in previous research can be discovered. However, simultaneous measurements of neuroimaging and pupillometry techniques are necessary to corroborate how pupil size and the activity of these neuromodulators, and possibly others, are related and interact during motor performance of variable emotionality.

AUTHOR CONTRIBUTIONS

Conceptualisation: M. V., K. E. O. and M. L.; data curation: M. V. and J. S.; formal analysis, M. V. and A. M. A.; funding acquisition: A. M. A. and M. L.; investigation: K. E. O. and J. S.; methodology: M. V. and K. E. O.; project administration: M. V., K. E. O.; resources: K. E. O. and J. S.; software: M. V.; supervision: A. M. A., P.-J. M., T. H. F. and M. L.; validation: M. V. and A. M. A.; visualisation: M. V.; writing—original draft: M.V.; writing—review & editing: M. V., T. H. F. and M. L. All authors read and approved the final manuscript.

ACKNOWLEDGEMENTS

We wish to thank Prof. Mark Cohen (UCLA Brain Research Institute) for providing valuable comments and suggestions on our study. We also would like to thank Prof. Gert Holstege, Prof. Chris Lowry and Prof. Arno Villringer for their contributions in discussions about the emotional motor system. We thank Kevin Smink for his help in making the supplementary animation video. Funding for open access charge: Max-Planck-Gesellschaft. Open Access funding enabled and organized by Projekt DEAL.

CONFLICT OF INTEREST STATEMENT


The authors declare no conflict of interest.

DATA AVAILABILITY STATEMENT

All data underlying the present findings are fully available and can be shared from M. V. upon request. Routines to compute the ROE algorithm are available online (<https://github.com/m-vidal/pupil-turbulence-removal>).

ORCID

Marc Vidal  <https://orcid.org/0000-0002-1084-3242>

Kelsey E. Onderdijk  <https://orcid.org/0000-0001-9992-7620>

Ana M. Aguilera  <https://orcid.org/0000-0003-2425-6716>

Joren Six  <https://orcid.org/0000-0001-7671-1907>

Pieter-Jan Maes  <https://orcid.org/0000-0002-9237-3298>

Thomas Hans Fritz  <https://orcid.org/0000-0003-1855-6026>

Marc Leman  <https://orcid.org/0000-0002-9780-2194>

PEER REVIEW

The peer review history for this article is available at <https://www.webofscience.com/api/gateway/wos/peer-review/10.1111/ejn.15998>.

REFERENCES

- Acal, C., Aguilera, A. M., Sarra, A., Evangelista, A., Battista, T. D., & Palermi, S. (2021). Functional ANOVA approaches for detecting changes in air pollution during the Covid-19 pandemic. *Stochastic Environmental Research and Risk Assessment*, *36*, 1083–1101.
- Albergaria, C., Silva, N. T., Pritchett, D. L., & Carey, M. R. (2018). Locomotor activity modulates associative learning in mouse cerebellum. *Nature Neuroscience*, *21*, 725–735.
- Arribas-Gil, A., & Romo, J. (2014). Shape outlier detection and visualization for functional data: The outliergram. *Biostatistics*, *15*(4), 603–619.
- Aston-Jones, G., & Cohen, J. D. (2005). An integrative theory of locus coeruleus-norepinephrine function: Adaptive gain and optimal performance. *Annual Review of Neuroscience*, *28*, 403–450.
- Auksztulewicz, R., & Friston, K. J. (2016). Repetition suppression and its contextual determinants in predictive coding. *Cortex*, *80*, 125–140.
- Ballinger, E. C., Ananth, M. R., Talmage, D. A., & Role, L. W. (2016). Basal forebrain cholinergic circuits and signaling in cognition and cognitive decline. *Neuron*, *91*, 1199–1218.
- Benarroch, E. E. (2009). The locus ceruleus norepinephrine system. *Neurology*, *73*(20), 1699–1704.
- Benarroch, E. E. (2021). *Cholinergic transmission, Neuroscience for clinicians: Basic processes, circuits, disease mechanisms, and therapeutic implications*. Oxford University Press.
- Bentley, P., Vuilleumier, P., Thiel, C. M., Driver, J., & Dolan, R. J. (2003a). Effects of attention and emotion on repetition priming and their modulation by cholinergic enhancement. *Journal of Neurophysiology*, *90*(2), 1171–1181.
- Bentley, P., Vuilleumier, P., Thiel, C. M., Driver, J., & Dolan, R. J. (2003b). Cholinergic enhancement modulates neural correlates of selective attention and emotional processing. *NeuroImage*, *20*, 58–70.
- Berridge, C. W. (2008). Noradrenergic modulation of arousal. *Brain Research Reviews*, *58*(1), 1–17.
- Blood, A. J., & Zatorre, R. J. (2001). Intensely pleasurable responses to music correlate with activity in brain regions implicated in reward and emotion. *Proceedings of the National Academy of Sciences of the United States of America*, *98*, 11818–11823.
- Bombeke, K., Duthoo, W., Mueller, S. C., Hopf, J.-M., & Boehler, C. N. (2016). Pupil size directly modulates the feedforward response in human primary visual cortex independently of attention. *NeuroImage*, *127*, 67–73.
- Breton-Provencher, V., & Sur, M. (2019). Active control of arousal by a locus coeruleus gabaergic circuit. *Nature Neuroscience*, *22*, 218–228.
- Brych, M., Murali, S., & Händel, B. (2021). How the motor aspect of speaking influences the blink rate. *PLoS One*, *16*(10), 1–19.
- Calderon, D. P., Kilinc, M., Maritan, A., Banavar, J. R., & Pfaff, D. W. (2016). Generalized CNS arousal: An elementary force within the vertebrate nervous system. *Neuroscience & Biobehavioral Reviews*, *68*, 167–176.
- Chang, A., Livingstone, S. R., Bosnyak, D. J., & Trainor, L. J. (2017). Body sway reflects leadership in joint music performance. *Proceedings of the National Academy of Sciences of the United States of America*, *114*, E4134–E4141.
- Christensen, W. F., & Zabriskie, B. N. (2021). When your permutation test is doomed to fail. *The American Statistician*, *76*, 53–63.
- de Gee, J. W., Colizoli, O., Kloosterman, N. A., Knapen, T. H. J., Nieuwenhuis, S., & Donner, T. H. (2017). Dynamic modulation of decision biases by brainstem arousal systems. *eLife*, *6*, e23232.
- Deco, G., & Kringelbach, M. L. (2020). Turbulent-like dynamics in the human brain. *Cell Reports*, *33*(10), 108471.
- Demiral, Ş. B., Liu, C. K., Benveniste, H., Tomasi, D., & Volkow, N. D. (2023). Activation of brain arousal networks coincident with eye blinks during resting state. *Cerebral Cortex*, bhad001. <https://doi.org/10.1093/cercor/bhad001>
- Demos, A. P., Chaffin, R., & Logan, T. (2018). Musicians body sway embodies musical structure and expression: A recurrence-based approach. *Musicae Scientiae*, *22*(2), 244–263.
- Duzel, E., & Guitart-Masip, M. (2013). Not so uncertain at last: Locus coeruleus and decision making. *Neuron*, *79*, 9–11.
- Escrachs, A., Perl, Y. S., Uribe, C., Camara, E., Türker, B., Pyatigorskaya, N., López-González, A., Pallavicini, C., Panda, R., Annen, J., Grosserries, O., Laureys, S., Naccache, L., Sitt, J. D., Laufs, H., Tagliazucchi, E., Kringelbach, M. L., & Deco, G. (2022). Unifying turbulent dynamics framework distinguishes different brain states. *Communications Biology*, *5*, 638.
- Everitt, B. J., & Robbins, T. W. (1997). Central cholinergic systems and cognition. *Annual Review of Psychology*, *48*, 649–684.
- Filipowicz, A., Glaze, C. M., Kable, J. W., & Gold, J. I. (2020). Pupil diameter encodes the idiosyncratic, cognitive complexity of belief updating. *eLife*, *9*, e57872.
- Friston, K. J., & Kiebel, S. J. (2009). Predictive coding under the free-energy principle. *Philosophical Transactions of the Royal Society B: Biological Sciences*, *364*, 1211–1221.
- Frühholz, S., Trost, W., & Grandjean, D. (2014). The role of the medial temporal limbic system in processing emotions in voice and music. *Progress in Neurobiology*, *123*, 1–17.
- Garey, J. D., Goodwillie, A. M., Frohlich, J., Morgan, M. A., Gustafsson, J.-A. A., Smithies, O., Korach, K. S., Ogawa, S., & Pfaff, D. W. (2003). Genetic contributions to generalized

- arousal of brain and behavior. *Proceedings of the National Academy of Sciences of the United States of America*, *100*, 11019–11022.
- Giordano, B. L., Whiting, C., Kriegeskorte, N., Kotz, S. A., Gross, J., & Belin, P. (2021). The representational dynamics of perceived voice emotions evolve from categories to dimensions. *Nature Human Behaviour*, *5*, 1203–1213.
- Harris, K. D., & Thiele, A. (2011). Cortical state and attention. *Nature Reviews Neuroscience*, *12*, 509–523.
- Hayashi, N., Someya, N., & Fukuba, Y. (2010). Effect of intensity of dynamic exercise on pupil diameter in humans. *Journal of Physiological Anthropology*, *29*, 119–122.
- Holstege, G., Bandler, R., & Saper, C. B. (1996). *The emotional motor system*, Progress in brain research: Elsevier.
- Holstege, G., & Subramanian, H. H. (2016). Two different motor systems are needed to generate human speech. *The Journal of Comparative Neurology*, *524*(8), 1558–1577.
- Jacques, J., & Preda, C. (2014). Model-based clustering for multivariate functional data. *Computational Statistics & Data Analysis*, *71*, 92–106.
- Jaffe, P. I., & Brainard, M. S. (2020). Acetylcholine acts on songbird premotor circuitry to invigorate vocal output. *eLife*, *9*, e53288.
- Joshi, S., & Gold, J. I. (2020). Pupil size as a window on neural substrates of cognition. *Trends in Cognitive Sciences*, *24*, 466–480.
- Joshi, S., Li, Y., Kalwani, R. M., & Gold, J. I. (2016). Relationships between pupil diameter and neuronal activity in the locus coeruleus, colliculi, and cingulate cortex. *Neuron*, *89*(1), 221–234.
- Kawashima, T., Shibusawa, S., & Amano, K. (2022). Frequency- and phase-dependent effects of auditory entrainment on attentional blink. *European Journal of Neuroscience*, *56*, 4411–4424.
- Knapen, T., de Gee, J. W., Brascamp, J., Nuiten, S., Hoppenbrouwers, S., & Theeuwes, J. (2016). Cognitive and ocular factors jointly determine pupil responses under equilibrium. *PLoS One*, *11*(5), 1–13.
- Knapen, T., & Gee, J. W. D. (2016). Firdeconvolution.
- Koelsch, S. (2014). Brain correlates of music-evoked emotions. *Nature Reviews Neuroscience*, *15*, 170–180.
- Koelsch, S., Vuust, P., & Friston, K. J. (2019). Predictive processes and the peculiar case of music. *Trends in Cognitive Sciences*, *23*, 63–77.
- Krishnamurthy, K., Nassar, M. R., Sarode, S., & Gold, J. I. (2017). Arousal-related adjustments of perceptual biases optimize perception in dynamic environments. *Nature Human Behaviour*, *1*, 107.
- Kuwamizu, R., Yamazaki, Y., Aoike, N., Ochi, G., Suwabe, K., & Soya, H. (2022). Pupil-linked arousal with very light exercise: Pattern of pupil dilation during graded exercise. *The Journal of Physiological Sciences*, *72*, 1–9.
- Leman, M. (2008). *Embodied music cognition and mediation technology*: MIT Press.
- Leman, M. (2016). *The expressive moment: How interaction (with music) shapes human empowerment*: MIT Press.
- Lévêque, Y., & Schön, D. (2015). Modulation of the motor cortex during singing-voice perception. *Neuropsychologia*, *70*, 58–63.
- Liebe, T., Kaufmann, J., Hämmerer, D., Betts, M. J., & Walter, M. (2022). In vivo tractography of human locus coeruleus–relation to 7t resting state FMRI, psychological measures and single subject validity. *Molecular Psychiatry*, *27*, 4984–4993.
- Liu, Y., Liang, X. S., & Weisberg, R. H. (2007). Rectification of the bias in the wavelet power spectrum. *Journal of Atmospheric and Oceanic Technology*, *24*, 2093–2102.
- Liu, X., Pfaff, D. W., Calderon, D. P., Tabansky, I., Wang, X., Wang, Y., & Kow, L. M. (2016). Development of electrophysiological properties of nucleus gigantocellularis neurons correlated with increased CNS arousal. *Developmental Neuroscience*, *38*, 295–310.
- Martin, E. M., Devidze, N., Shelley, D. N., Westberg, L., Fontaine, C., & Pfaff, D. W. (2011). Molecular and neuroanatomical characterization of single neurons in the mouse medullary gigantocellular reticular nucleus. *The Journal of Comparative Neurology*, *519*, 2574–2593.
- Martin, J. T., Whittaker, A. H., & Johnston, S. J. (2020). Component processes in free-viewing visual search: Insights from fixation-aligned pupillary response averaging. *Journal of Vision*, *20*, 5–5.
- McDougal, D. H., & Gamlin, P. D. (2015). Autonomic control of the eye. *Comprehensive Physiology*, *5*(1), 439–473.
- McGaugh, J. D. (2004). The amygdala modulates the consolidation of memories of emotionally arousing experiences. *Annual Review of Neuroscience*, *27*, 1–28.
- McGinley, M. J., Vinck, M., Reimer, J., Batista-Brito, R., Zaghera, E., Cadwell, C. R., Tolias, A. S., Cardin, J. A., & McCormick, D. A. (2015). Waking state: Rapid variations modulate neural and behavioral responses. *Neuron*, *87*(6), 1143–1161.
- McGowan, A. L., Chandler, M. C., Brascamp, J. W., & Pontifex, M. B. (2019). Pupillometric indices of locus-coeruleus activation are not modulated following single bouts of exercise. *International Journal of Psychophysiology*, *140*, 41–52.
- Megemont, M., Mcburney-lin, J., & Yang, H. (2022). Pupil diameter is not an accurate real-time readout of locus coeruleus activity. *eLife*, *11*, e70510.
- Montefusco-Siegmund, R., Schwalm, M., Jubal, E. R., Devia, C., Egaña, J. I., & Maldonado, P. E. (2022). Alpha eeg activity and pupil diameter coupling during inactive wakefulness in humans. *eNeuro*, *9*(2), ENEURO.0060-21.2022.
- Murphy, P. R., O'Connell, R. G., O'Sullivan, M., Robertson, I. H., & Balsters, J. H. (2014). Pupil diameter covaries with bold activity in human locus coeruleus. *Human Brain Mapping*, *35*(8), 4140–4154.
- Naber, M., Alvarez, G. A., & Nakayama, K. (2013). Tracking the allocation of attention using human pupillary oscillations. *Frontiers in Psychology*, *4*, 919.
- Naber, M., Hommel, B., & Colzato, L. S. (2015). Improved human visuomotor performance and pupil constriction after choline supplementation in a placebo-controlled double-blind study. *Scientific Reports*, *5*, 1–9.
- Naber, M., & Murphy, P. R. (2019). Pupillometric investigation into the speed-accuracy trade-off in a visuo-motor aiming task. *Psychophysiology*, *57*, e13499.
- Nassar, M. R., Rumsey, K. M., Wilson, R. C., Parikh, K., Heasly, B. S., & Gold, J. I. (2012). Rational regulation of learning dynamics by pupil-linked arousal systems. *Nature Neuroscience*, *15*, 1040–1046.
- Nelson, A., & Mooney, R. (2016). The basal forebrain and motor cortex provide convergent yet distinct movement-related inputs to the auditory cortex. *Neuron*, *90*, 635–648.

- Norman-Haignere, S. V., Feather, J., Boebinger, D., Brunner, P., Ritaccio, A. L., McDermott, J. H., Schalk, G., & Kanwisher, N. G. (2022). A neural population selective for song in human auditory cortex. *Current Biology*, *32*, 1470–1484.e12.
- Nussek, M., & Wanderley, M. M. (2009). Music and motion: How music-related ancillary body movements contribute to the experience of music. *Music Perception*, *26*, 335–353.
- Pachitariu, M., Lyamzin, D. R., Sahani, M., & Lesica, N. A. (2015). State-dependent population coding in primary auditory cortex. *The Journal of Neuroscience*, *35*, 2058–2073.
- Peysakhovich, V., Causse, M., Scannella, S., & Dehais, F. (2015). Frequency analysis of a task-evoked pupillary response: Luminance-independent measure of mental effort. *International Journal of Psychophysiology*, *97*(1), 30–37.
- Pfaff, D. W. (2009). *Brain arousal and information theory: Neural and genetic mechanisms*: Harvard University Press.
- Pfaff, D. W., Martin, E. M., & Faber, D. S. (2012). Origins of arousal: Roles for medullary reticular neurons. *Trends in Neurosciences*, *35*, 468–476.
- Pfaff, D. W., Ribeiro, A. C., Matthews, J., & Kow, L. M. (2008). Concepts and mechanisms of generalized central nervous system arousal. *Annals of the New York Academy of Sciences*, *1129*, 11–25.
- Picciotto, M. R., Higley, M. J., & Mineur, Y. S. (2012). Acetylcholine as a neuromodulator: Cholinergic signaling shapes nervous system function and behavior. *Neuron*, *76*, 116–129.
- Pinto, L., Goard, M. J., Estandian, D., Xu, M., Kwan, A., Lee, S.-H., Harrison, T. C., Feng, G., & Dan, Y. (2013). Fast modulation of visual perception by basal forebrain cholinergic neurons. *Nature Neuroscience*, *16*, 1857–1863.
- Quinkert, A. W., Vimal, V. P., Weil, Z. M., Reeke, G. N., Schiff, N. D., Banavar, J. R., & Pfaff, D. W. (2011). Quantitative descriptions of generalized arousal, an elementary function of the vertebrate brain. *Proceedings of the National Academy of Sciences of the United States of America*, *108*, 15617–15623.
- R Core Team (2021). R: A language and environment for statistical computing. In *R Foundation for Statistical Computing*, Vienna, Austria.
- Ramsay, J., & Silverman, B. W. (2005). *Functional data analysis*. New York: Springer.
- Reimer, J., Froudarakis, E., Cadwell, C. R., Yatsenko, D., Denfield, G. H., & Tolias, A. S. (2014). Pupil fluctuations track fast switching of cortical states during quiet wakefulness. *Neuron*, *84*, 355–362.
- Reimer, J., McGinley, M. J., Liu, Y., Rodenkirch, C., Wang, Q., McCormick, D. A., & Tolias, A. S. (2016). Pupil fluctuations track rapid changes in adrenergic and cholinergic activity in cortex. *Nature Communications*, *7*, 13289.
- Ross, J. M., Comstock, D. C., Iversen, J. R., Makeig, S., & Balasubramaniam, R. (2021). Cortical mu rhythms during action and passive music listening. *Journal of Neurophysiology*, *127*, 213–224.
- Sakata, S. (2016). State-dependent and cell type-specific temporal processing in auditory thalamocortical circuit. *Scientific Reports*, *6*, 18873.
- Sánchez-Islas, M., Toledo-Roy, J. C., & Frank, A. (2021). Criticality in a multisignal system using principal component analysis. *Physical Review E*, *103* 4-1, 42111.
- Sara, S. (2009). The locus coeruleus and noradrenergic modulation of cognition. *Nature Reviews Neuroscience*, *10*, 211–223.
- Scherer, K. R., Sundberg, J., Fantini, B., Trznadel, S., & Eyben, F. (2017). The expression of emotion in the singing voice: Acoustic patterns in vocal performance. *The Journal of the Acoustical Society of America*, *142*, 1805.
- Schmidt, G., Malik, M., Barthel, P., Schneider, R., Ulm, K., Rolnitzky, L., Camm, A. J., Bigger, J. T., & Schömig, A. (1999). Heart-rate turbulence after ventricular premature beats as a predictor of mortality after acute myocardial infarction. *The Lancet*, *353*(9162), 1390–1396.
- Schwabe, L., Merz, C. J., Walter, B., Vaitl, D., Wolf, O. T., & Stark, R. (2011). Emotional modulation of the attentional blink: The neural structures involved in capturing and holding attention. *Neuropsychologia*, *49*, 416–425.
- Schwartz, J. W., Sanchez, M. M., & Gouzoules, H. (2022). Vocal expression of emotional arousal across two call types in young rhesus macaques. *Animal Behaviour*, *190*, 125–138.
- Shigeta, T. T., Morris, T. P., D.L. Hartwell, C. J. K. H., Kucyi, A., Bex, P. J., Kramer, A. F., & Hillman, C. H. (2021). Acute exercise effects on inhibitory control and the pupillary response in young adults. *International Journal of Psychophysiology*, *170*, 218–228.
- Staib, M., & Frühholz, S. (2021). Cortical voice processing is grounded in elementary sound analyses for vocalization relevant sound patterns. *Progress in Neurobiology*, *200*, 101982.
- Tabansky, I., Liang, Y., Frankfurt, M., Daniels, M. A., Harrigan, M., Stern, S. A., Milner, T. A., Leshan, R. L., Rama, R., Moll, T., Friedman, J. M., Stern, J. N. H., & Pfaff, D. W. (2018). Molecular profiling of reticular gigantocellularis neurons indicates that ENOS modulates environmentally dependent levels of arousal. *Proceedings of the National Academy of Sciences of the United States of America*, *115*, E6900–E6909.
- Torrence, C., & Compo, G. P. (1998). A practical guide to wavelet analysis. *Bulletin of the American Meteorological Society*, *79*, 61–78.
- Vazey, E. M., Moorman, D. E., & Aston-Jones, G. (2018). Phasic locus coeruleus activity regulates cortical encoding of salience information. *Proceedings of the National Academy of Sciences of the United States of America*, *115*, E9439–E9448.
- Vidal, M., & Aguilera, A. M. (2023). Novel whitening approaches in functional settings. *Stat*, *12*(1), e516.
- Vinck, M. A., Batista-Brito, R. A., Knoblich, U., & Cardin, J. A. (2015). Arousal and locomotion make distinct contributions to cortical activity patterns and visual encoding. *Neuron*, *86*, 740–754.
- Wang, C.-A., & Munoz, D. P. (2015). A circuit for pupil orienting responses: Implications for cognitive modulation of pupil size. *Current Opinion in Neurobiology*, *33*, 134–140.
- White, O., & French, R. (2017). Pupil diameter may reflect motor control and learning. *Journal of Motor Behavior*, *49*, 141–149.
- Yoo, K., Ahn, J., & Lee, S.-H. (2021). The confounding effects of eye blinking on pupillometry, and their remedy. *PLoS One*, *16*(12), 1–32.

- Zénon, A., Sidibé, M., & Olivier, E. (2014). Pupil size variations correlate with physical effort perception. *Frontiers in Behavioral Neuroscience*, 8, 286.
- Zhou, R., Liu, J., Kumar, S., & Palomar, D. P. (2020). Student's *t*-VAR modeling with missing data via stochastic em and Gibbs sampling. *IEEE Transactions on Signal Processing*, 68, 6198–6211.

SUPPORTING INFORMATION

Additional supporting information can be found online in the Supporting Information section at the end of this article.

How to cite this article: Vidal, M., Onderdijk, K. E., Aguilera, A. M., Six, J., Maes, P.-J., Fritz, T. H., & Leman, M. (2023). Cholinergic-related pupil activity reflects level of emotionality during motor performance. *European Journal of Neuroscience*, 1–15. <https://doi.org/10.1111/ejn.15998>